

Characterization of hot solar-type stars with exoplanets

Yuri Damasceno¹

University of Porto, Rua do Campo Alegre s/n, 4169-007 Porto
e-mail: ¹up201908108@up.pt

August 5, 2022

ABSTRACT

Aims. The goals for this project were to obtain a general method for spectral analysis to determine stellar atmosphere parameters of solar-type stars in the temperature range [6100,7200]K with exoplanets using the spectral analysis software iSpec. We use this method to determine the stellar effective temperature, surface gravity, metallicity, alpha element abundance, microturbulence, macroturbulence and projected rotational velocity.

Methods. Using iSpec we treat all spectra correcting their radial velocity and applying a normalization. Using a list of the FeI and FeII iron lines we execute an initial synthetic spectral fit. This can be improved by discarding from the line list lines that are not correctly reproduced, reducing the initial line list. Using the reduced line lists we derive stellar atmosphere parameters following the MARCS atmosphere models and using the radiative transfer codes Turbospectrum, Synthe and MOOG.

Results. We reached 2 reduced line lists and derived the stellar parameters for all 6 stars. We tested and obtained a general and consistent spectral analysis procedure for hot solar-type stars with exoplanets such that it can be easily reproducible. We analysed and derived stellar parameters for the stars HD 1666, HD103774, HD11231, HD 156846, WASP-101 and WASP-190.

Key words. Exoplanets – Spectroscopy – Stellar Parameters – iSpec

1. Introduction

The spectra of stars is a commonly used mean to study its characteristics and properties. Throughout the years several tools for spectral analysis have been developed in order to derive these properties with greater accuracy, efficiency and consistency (Blanco-Cuaresma et al. (2014)). This analysis is done by relating the shape of the absorption lines with a set of stellar parameters that accurately matches the observed spectra. Within this area there are different approaches on how to process the data. One of these methods, which was used in this work, is the spectral synthesis method. This method consists of producing a synthetic theoretical spectrum using a set of stellar parameters (Sousa (2014)). A final result is obtained when the synthetic spectrum matches the observed one, returning the corresponding parameters for that star. This process can however become harder for hot stars with high rotational velocity, since absorption lines are more likely to overlap thus creating a less clear spectrum to fit.

The process of creating synthetic spectra and searching for the best fit is done computationally, existing many codes to carry on this work. We will use 3 of these: Turbospectrum (Plez (2012)), Synthe (Kurucz (2005)) and MOOG (Sneden et al. (2012)). In this project we intended to compare these radiative transfer codes using the spectral analysis software, iSpec (Blanco-Cuaresma et al. (2014)), for stars with exoplanets within the temperature range [6100, 7200] K, in order to determine the parameters: effective temperature (T_{eff}), surface gravity ($\log(g)$), iron abundance ($[Fe/H]$), microturbulence (ξ), macroturbulence (v_{mac}), alpha element abundance ($[\alpha/Fe]$) and the projected rotational velocity ($v \sin(i)$).

2. Principles of Spectroscopy

The basis of spectroscopy dates back to Newton's prism, where a beam of light can be decomposed into its continuum of frequency components. For our purposes, the light emitted from stars can be decomposed into their respective signature spectra. The multiple absorption lines can provide information of the stars properties, given these relate with the depth and width of the lines.

Stars with a high effective temperature and projected rotational velocity present a challenge for spectral analysis, since the broadening of the lines is higher resulting in the merging of consecutive lines. Most codes struggle in such situations as it becomes much more difficult to distinguish individual lines and to determine a clear set of parameters that matches the observed spectrum. In order to obtain trustworthy results a sequence of procedures must be taken to minimize the sources of error and ambiguity. All these steps were done using iSpec for each of the spectra analysed throughout this work.

3. Data preparation

3.1. Importing data and errors

The spectra was viewed and analysed using iSpec. From the provided spectrum, in the cases where the errors were not initially defined we determined them within the software. This estimate is based on the signal to noise ratio (SNR), which can be calculated directly from iSpec through a designated function. Having the values of SNR, represented in table 1 we set the error for each point as the inverse of the SNR multiplied by the flux at that point. This operation can also be done within iSpec. We analysed the spectra of 6 stars, all hosting 1 known exoplanet each¹:

¹ exoplanet.eu

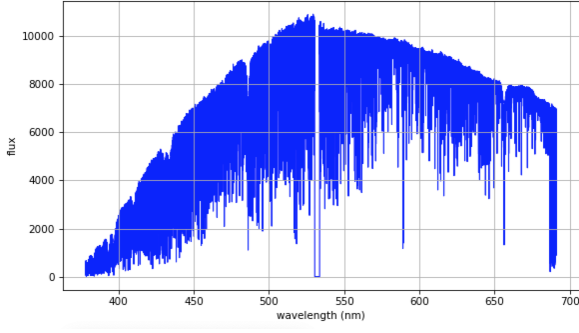


Fig. 1: Spectra of HD 1666 before being reduced and normalized.

- HD1666, spectral type F7
- HD103774, spectral type F5
- HD11231, spectral type F5
- HD156846, spectral type G0
- WASP-101, spectral type F6
- WASP-190, spectral type F6

All spectra were obtained by the spectrograph HARPS, which has a resolution of 115000 and a wavelength range of 380 to 690 nm (Mayor et al. (2003)) (which contains the ranges used throughout this work). The reference values for the effective temperature, surface gravity, metallicity and microturbulence were taken from the SWEET-Cat catalogue (Sousa & et al. (2021)) and are shown in tale 2.

Table 1: SNR values for studied stars determined within iSpec. The first two values were given and the remaining determined in iSpec.

	HD 1666	HD 103774	HD 11231	HD 156846	WASP-101	WASP-190
SNR	120	800	365.54	309.58	221.79	109.08

Table 2: Reference values for T_{eff} , $\log(g)$, $[Fe/H]$ and ξ reported in SWEET-Cat.

	T_{eff} (K)		$\log(g)$ (dex)		$[Fe/H]$ (dex)		ξ (km/s)	
	value	error	value	error	value	error	value	error
HD 1666	6508	30	4.29	0.03	0.39	0.02	1.77	0.03
HD 103774	6586	35	4.48	0.03	0.31	0.02	1.72	0.02
HD 11231	6643	35	4.32	0.04	0.19	0.02	1.96	0.04
HD 156846	6152	20	4.16	0.04	0.23	0.02	1.45	0.02
WASP-101	6604	50	4.77	0.04	0.31	0.03	1.84	0.07
WASP-190	6730	55	4.52	0.07	0.15	0.04	2.07	0.09

3.2. Normalization of spectrum

The first step is to prepare the data, starting with a normalization of the spectrum to correctly measure the characteristic quantities of the absorption lines (width, depth, etc.). Normalization consists of dividing every wavelength point by the theoretical flux if there were no lines, such that the continuum is fixed at flux=1, and the lines all fall below this value.

The stars continuum curve depends on the effective temperature, having a larger flux at certain wavelengths, thus we must determine it by approximating the curve with non-linear functions. iSpec has a function for fitting the continuum using splines, as well as other methods, and suggests based on the data the parameters of the fit. Using the default parameters, however,

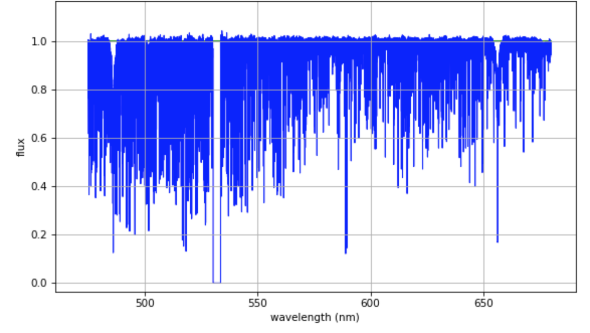


Fig. 2: Spectra of HD 1666 after reduced and normalized using 60 splines and a wavelength step of 0.05 nm for median selection and of 4 nm for maximum selection.

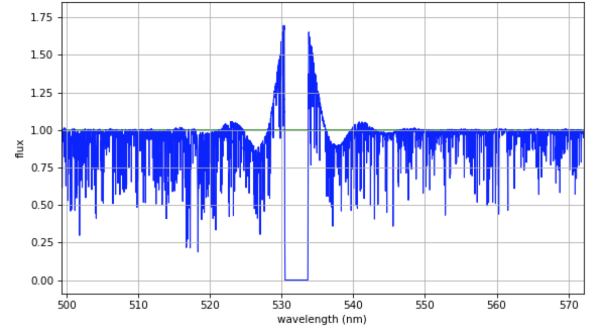


Fig. 3: Bad normalization in the spectrum of HD 103774 near the section without data.

results in a bad fit around the region without data for some of the stars, as can be seen in figure 3, for example.

For all spectra we fit the continuum with 60 splines and a wavelength step of 0.05 nm for median selection and of 4 nm for maximum selection. The remaining parameters were left as default. This allows for a smooth continuum fit, even near the area without data, which previously did not normalize correctly.

The following step is to correct the radial velocity relative to the atomic lines. Due to the movement of the star, absorption lines appear shifted, as their central wavelength changes relative to the expected central value for each peak. From this shift we can estimate the radial velocity of the star and correct the spectrum for that value. From iSpec this estimate can be made using all default parameters (using option Parameters -> Determine velocity relative to... -> atomic line mask), which yields the values in table 3. Once determined, we can set the error by using the option Operations -> Correct velocity relative to... -> atomic line mask.

Table 3: Mean velocity and error relative to atomic lines estimated by the deviation between the peak central wavelength and the expected wavelength.

	HD1666	HD103774	HD11231	HD156846	WASP-101	WASP-190
mean v (km/s)	17.85	-3.07	7.47	-68.27	42.65	1.05
error (km/s)	0.04	0.07	0.05	0.03	0.12	0.18

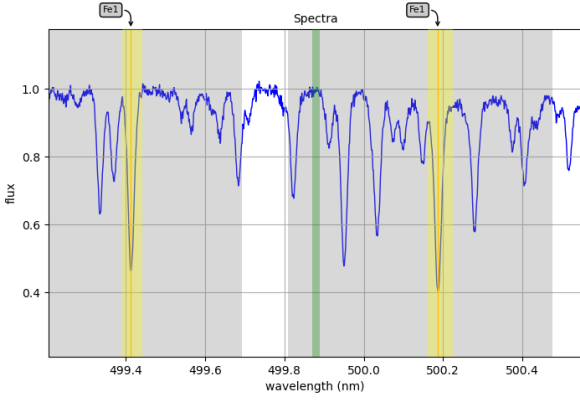


Fig. 4: A section of the spectrum visualized on iSpec, with the segment in grey, line regions in yellow (corresponding to 2 *FeI* lines as stated by the labels) and continuum regions in green.

3.3. Defining continuum and line regions

We then must define the continuum and line regions. We used the lines corresponding to atomic iron *FeI* and ionized iron *FeII*, as well as a list of continuum regions (regions without any lines). In iSpec both must be inserted into segments, as shown in figure 4. All these lists are provided after downloading the software (these can be found in the input \rightarrow regions folder). We note that the HARPS spectra has a data gap between 530.4 and 533.7 nm without data, thus we removed all line regions within it. The line and continuum lists used only cover a portion of the full spectra, so we cropped it to leave only the data between 475 to 680 nm. This reduction doesn't affect the fitting since the codes used only evaluate the fit in the line regions. Outside the line regions the differences between the fit and the data don't matter, however reducing the wavelength range can help with the normalization of the spectra.

4. Synthetic spectrum fitting

4.1. Initial parameters

Creating a synthetic spectra involves an iterative χ^2 minimization process, thus the initial parameters must be inputted prior to the fitting. Since we are using spectra from HARPS we used a fixed resolution of 115000, leaving the values for T_{eff} , $\log(g)$, $[Fe/H]$, ξ , $[\alpha/Fe]$ and $v \sin(i)$ free to vary from the default values filled by iSpec², and determining the macroturbulence v_{mac} using the empiric formula shown in equation 1 (Doyle et al. (2014)). This formula was modified from the original, in the iSpec script `common.py` in line 974. The limb darkening coefficient was treated as fixed, at 0.6 for all stars, as well as the resolution, set to 115000. For all codes and stars we used the MARCS model atmospheres (Gustafsson et al. (2008)), returning the stellar parameters after 6 iterations. The computational time for these conditions varies from code to code, taking on average 10 minutes for MOOG and between 1 and 2 hours for Turbospectrum and Synthe.

$$v_{mac} = 3.21 - 2.33 \times 10^{-3}(T_{eff} - 5777) + 2.00 \times 10^{-6}(T_{eff} - 5777)^2 - 2(\log(g) - 4.44) \quad (1)$$

² The default values are: $T_{eff} = 5771$, $\log(g) = 4.44$, $[Fe/H] = 0$, $\xi = 1.05$, $[\alpha/Fe] = 0$ and $v \sin(i) = 1.6$

4.2. First fit and line selection

It is essential to select the lines more suitable for the synthesis, as some of them may be overlapping neighbour lines or have too much noise and an unclear shape. We executed a first synthesis using the codes Turbospectrum, Synthe and MOOG, using the full iron line list and from the resulting synthetic spectrum we evaluated individually the lines to be removed. Once the line list has been filtered we run the codes once more.

It is possible, and was the case for some stars such as WASP-101, that the first fit does not return results for some codes, if not all. This happens for spectra that are very hard to read, with many overlapped lines and noisy data. In this case we must view each case and manually filter the lines, judging if each line is well defined, isolated and fitted. Examples of cases where lines were removed are illustrated in figure ?? in the annexes.

The procedure of reducing the line list after a first fit was done for stars HD 1666 and HD 103774, individually treated, resulting in 2 slightly different reduced line lists. Using a python script and the 2 line lists, we can create a new line list containing the common lines between the originally provided lists, which will be equal or smaller than these.

4.3. Reduced line lists

Using the line list created from intercepting the HD 1666 selection and the HD 103774 selection we can now use it to obtain the stellar parameters of the remaining 4 stars, as well as test if this list is capable of returning satisfactory results. In cases where the list failed to return results for more than one code, we executed yet another selection process. This was the case for WASP-101, for which after removing additional lines we obtained the second reduced line list. The original iron lists list provided with iSpec has 315 line regions, the first line list was reduced to 142 regions and the second to 105 regions³.

5. Results

Using codes Turbospectrum, Synthe and MOOG and the first and second reduced line lists, we were able to reach the results presented in tables B.1 to B.6.

For each fit, we present the χ^2 and the RMS errors. The entries without values represent cases where the code failed to fit the spectrum. WASP-101 showed to be a particularly challenging spectrum since no code was able to fit the spectrum using the first line list, as verified from table B.5, thus the necessity for a second reduction. From tables B.5 and B.6 we notice Synthe was not able to fit for any line list. This can show this code does not perform as well for stars with a very high rotational velocity. In all cases Turbospectrum returned results, showing to be a more stable code. MOOG doesn't fall short, only failing for HD 103774. All successful runs present a χ^2 below 5 and an RMS below 0.025. The general uncertainties are below those from the reference values in table 2.

The difference graphs show MOOG tends to estimate higher values for T_{eff} , $\log(g)$ and $[Fe/H]$, followed by Turbospectrum, with Synthe returning the lowest estimates for these parameters. All codes fit the spectra by balancing these differences with

³ The final lists and altered iSpec code `common.py` can be found in <https://github.com/ChickenWithBeans/Line-lists-for-spectral-analysis-of-Hot-Solar-type-stars-with>

⁴ Star color code: HD1666:blue, HD103774:green, HD11231:orange, HD156846:yellow, WASP-101:purple, WASP-190:grey.

⁴ http://stev.oapd.inaf.it/cgi-bin/cmd_3.6

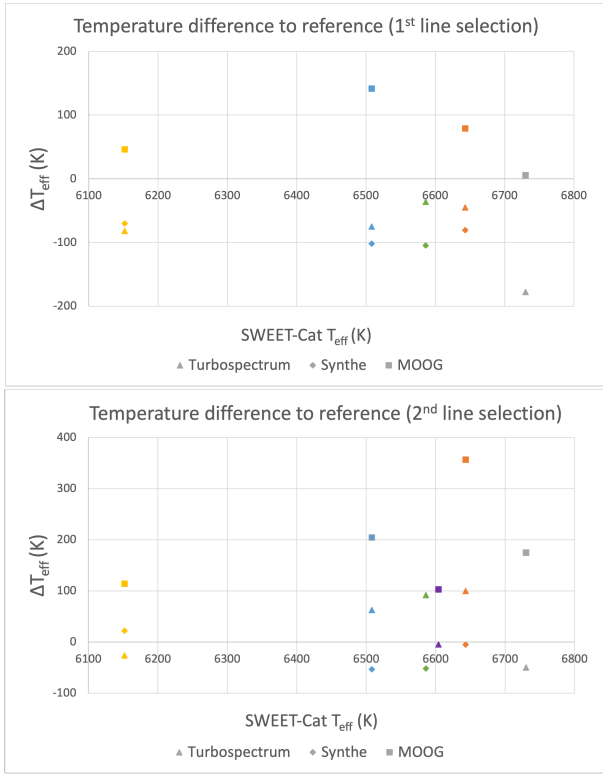


Fig. 5: Difference between obtained effective temperatures and the reference values for all codes (distinguished by shape) and all stars (distinguished by colour)⁴ using the first reduced line list (top) and the second reduced line list (bottom).

$v \sin(i)$. From the results we can notice MOOG has the lowest estimates for $v \sin(i)$ and Synthe the highest, with Turbospectrum in the middle.

The second line list as well results in higher estimates for all codes in the majority of cases. The uncertainties are higher for the second line list, likely due to the lower number of lines. The first line list failed in 5 out of the 18 runs, while the second line list failed in 3.

6. Conclusions

We present the stellar atmosphere parameters for the 6 hot solar-type stars with exoplanets using a general method for the spectral analysis through the software iSpec and the codes Turbospectrum, Synthe and MOOG. Turbospectrum presented to be the most stable code for the least failure rate and Synthe showed higher failure for fast rotating stars. Amongst the radiative codes tested, the temperature values are usually estimated to be highest using MOOG and lowest using Synthe, with the rotational velocity following the opposite tendency.

We defined 2 line lists composed of a selection of FeI and FeII iron lines for general use with the synthesis method for hot solar-type stars. We found the second line list returns higher estimates for the temperature, surface gravity and metallicity, resulting in lower estimates for the rotational velocity. Due to the reduced number of line regions, the second list presents higher uncertainties however a lower failure rate.

The results were obtained using a consistent and homogeneous data treatment and analysis, thus making them easily reproducible.

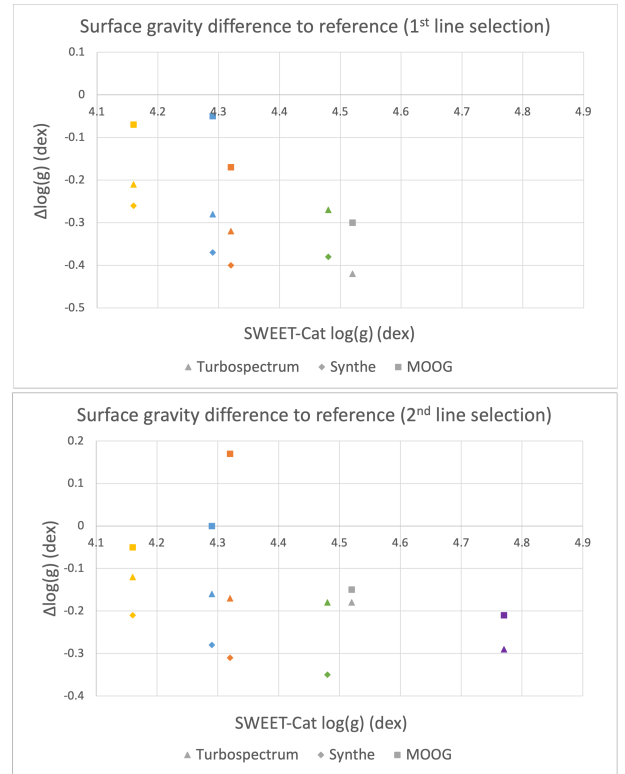


Fig. 6: Difference between obtained surface gravities and the reference values for all codes (distinguished by shape) and all stars (distinguished by colour)³ using the first reduced line list (top) and the second reduced line list (bottom).

References

- Blanco-Cuaresma, S., Soubiran, C., Heiter, U., & Jofré, P. 2014, A&A, 569, A111
- Doyle, A. P., Davies, G. R., Smalley, B., Chaplin, W. J., & Elsworth, Y. 2014, MNRAS, 444, 3592
- Gustafsson, B., Edvardsson, B., Eriksson, K., et al. 2008, A&A, 486, 951
- Kurucz, R. L. 2005, Memorie della Societa Astronomica Italiana Supplementi, 8, 14
- Mayor, M., Pepe, F., Queloz, D., et al. 2003, The Messenger, 114, 20
- Plez, B. 2012, Turbospectrum: Code for spectral synthesis, Astrophysics Source Code Library, record ascl:1205.004
- Snedden, C., Bean, J., Ivans, I., Lucatello, S., & Sobeck, J. 2012, MOOG: LTE line analysis and spectrum synthesis, Astrophysics Source Code Library, record ascl:1202.009
- Sousa, S. G. 2014, in Determination of Atmospheric Parameters of B, 297–310
- Sousa, S. G. & et al. 2021, A&A, 656, A53

Acknowledgements. This project was supervised by Sérgio Sousa and Elisa Delgado-Mena

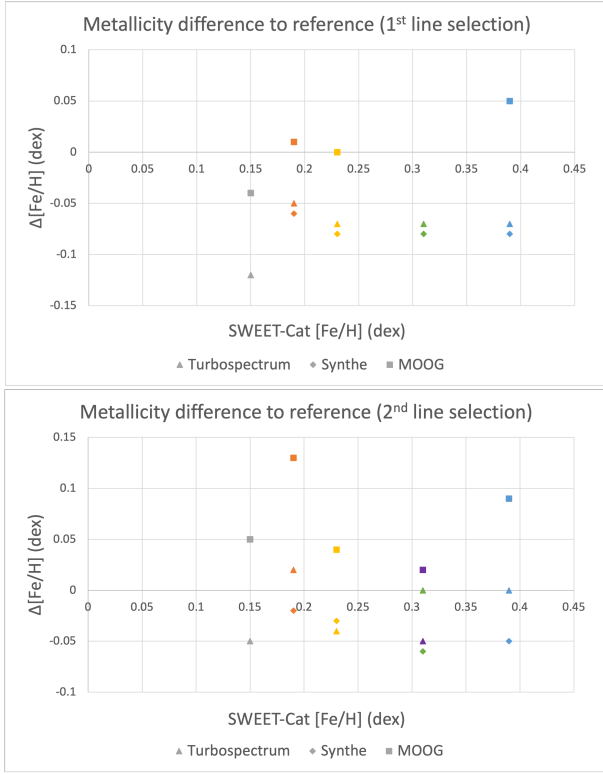


Fig. 7: Difference between obtained metallicities and the reference values for all codes (distinguished by shape) and all stars (distinguished by color)³ using the first reduced line list (top) and the second reduced line list (bottom).

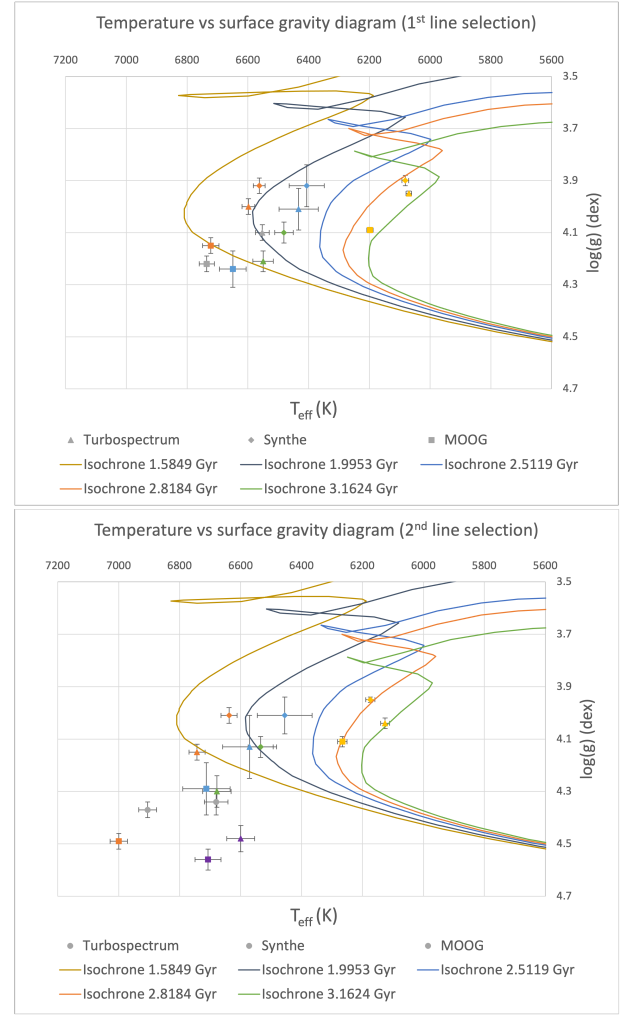


Fig. 8: Display of the effective temperature and surface gravity for all codes (distinguished by shape) and all stars (distinguished by color)³ on a T_{eff} vs $\log(g)$ diagram, using the first reduced line list (top) and the second reduced line list (bottom). The shown curves are the PARSEC tracks for metallicity of 0.166 and various ages⁴.

Appendix A: Additional Figures

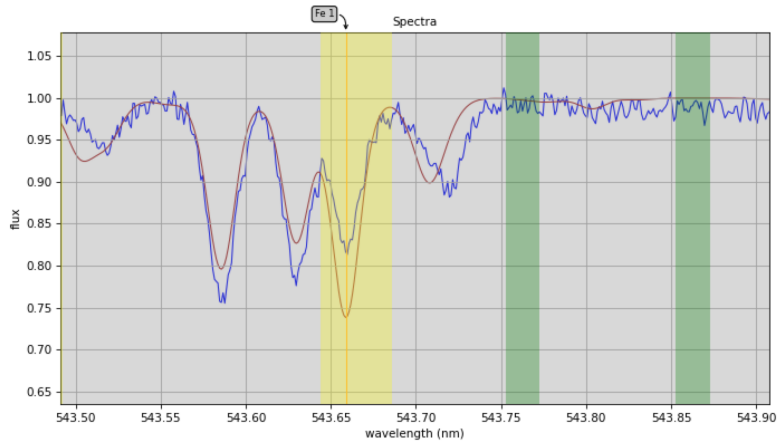


Fig. A.1: Example from HD 1666 spectrum of an excluded line region due to bad match between fitted line and observed line. The blue graph represents the observed spectrum and the red graph represents the fitted synthetic spectrum.

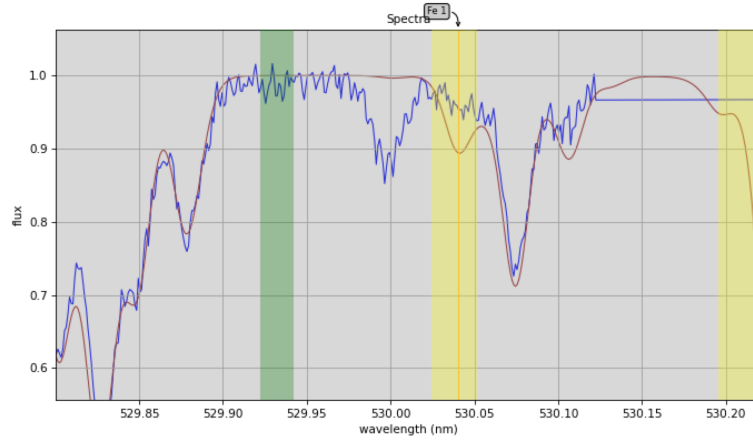


Fig. A.2: Examples from HD 1666 spectrum of an excluded line region due to very noisy data. The blue graph represents the observed spectrum and the red graph represents the fitted synthetic spectrum.

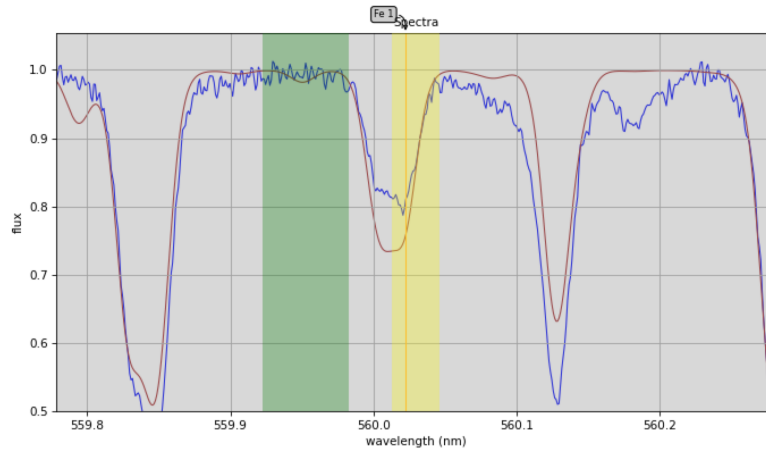


Fig. A.3: Examples from HD 1666 spectrum of an excluded line region due to peak overlapping of multiple lines. The blue graph represents the observed spectrum and the red graph represents the fitted synthetic spectrum.

Appendix B: Results Tables

Table B.1: Results obtained for HD 1666 with the first reduced line list (top table) and for the second reduced line list (bottom table).

		T_{eff} (K)		$\log(g)$ (dex)		$[Fe/H]$ (dex)		$[\alpha/Fe]$ (dex)		ξ (km/s)		v_{mac} (km/s)		$v\sin(i)$ (km/s)		χ^2	RMS
		value	error	value	error	value	error	value	error	value	error	value	error	value	error		
First reduced	Turbospec	6433	64	4.01	0.08	0.32	0.03	-0.04	0.11	1.73	0.06	6.46	empirical	5.34	0.26	4.89	0.0239
	Synthe	6406	58	3.92	0.08	0.31	0.03	0.01	0.10	1.72	0.06	6.51	empirical	5.30	0.28	4.93	0.024
	MOOG	6650	44	4.24	0.07	0.44	0.03	0.00	0.12	1.81	0.06	7.17	empirical	4.53	0.26	5.13	0.0244
Second reduced	Turbospec	6571	88	4.13	0.12	0.39	0.04	0.02	0.11	1.75	0.08	6.93	empirical	4.72	0.45	3.29	0.0221
	Synthe	6455	90	4.01	0.07	0.34	0.04	0.03	0.10	1.72	0.09	6.57	empirical	5.23	0.21	3.67	0.0233
	MOOG	6712	78	4.29	0.10	0.48	0.04	-0.04	0.13	1.81	0.07	7.44	empirical	4.20	0.54	3.59	0.023

Table B.2: Results obtained for HD 103774 with the first reduced line list (top table) and for the second reduced line list (bottom table).

		T_{eff} (K)		$\log(g)$ (dex)		$[Fe/H]$ (dex)		$[\alpha/Fe]$ (dex)		ξ (km/s)		v_{mac} (km/s)		$v\sin(i)$ (km/s)		χ^2	RMS
		value	error	value	error	value	error	value	error	value	error	value	error	value	error		
First reduced	Turbospec	6550	34	4.21	0.04	0.24	0.02	-0.12	0.06	1.62	0.04	6.67	empirical	8.56	0.11	1.99	0.0152
	Synthe	6481	31	4.10	0.04	0.23	0.02	-0.13	0.05	1.61	0.04	6.52	empirical	8.65	0.10	1.93	0.015
	MOOG	-	-	-	-	-	-	-	-	-	-	-	-	-	-	-	-
Second reduced	Turbospec	6678	47	4.30	0.06	0.31	0.02	-0.08	0.06	1.66	0.05	7.21	empirical	8.23	0.17	1.17	0.0132
	Synthe	6534	41	4.13	0.04	0.25	0.02	-0.09	0.05	1.64	0.05	6.73	empirical	8.53	0.15	1.31	0.0139
	MOOG	-	-	-	-	-	-	-	-	-	-	-	-	-	-	-	-

Table B.3: Results obtained for HD 11231 with the first reduced line list (top table) and for the second reduced line list (bottom table).

		T_{eff} (K)		$\log(g)$ (dex)		$[Fe/H]$ (dex)		$[\alpha/Fe]$ (dex)		ξ (km/s)		v_{mac} (km/s)		$v\sin(i)$ (km/s)		χ^2	RMS
		value	error	value	error	value	error	value	error	value	error	value	error	value	error		
First reduced	Turbospec	6598	21	4.00	0.03	0.14	0.01	-0.08	0.05	1.85	0.02	7.35	empirical	6.41	0.09	2.71	0.0178
	Synthe	6562	19	3.92	0.03	0.13	0.01	-0.04	0.04	1.82	0.02	7.30	empirical	6.45	0.09	2.71	0.0178
	MOOG	6722	27	4.15	0.03	0.20	0.01	-0.03	0.04	1.89	0.03	7.77	empirical	6.09	0.15	2.94	0.0185
Second reduced	Turbospec	6743	26	4.15	0.03	0.21	0.01	-0.02	0.04	1.89	0.03	7.90	empirical	5.80	0.18	1.76	0.0161
	Synthe	6638	27	4.01	0.03	0.17	0.01	-0.01	0.04	1.85	0.03	7.56	empirical	6.18	0.16	1.99	0.0171
	MOOG	7000	28	4.49	0.03	0.32	0.01	0.00	0.04	1.93	0.03	8.95	empirical	4.23	0.28	2.09	0.0176

Table B.4: Results obtained for HD 156846 with the first reduced line list (top table) and for the second reduced line list (bottom table).

		T_{eff} (K)		$\log(g)$ (dex)		$[Fe/H]$ (dex)		$[\alpha/Fe]$ (dex)		ξ (km/s)		v_{mac} (km/s)		$v\sin(i)$ (km/s)		χ^2	RMS
		value	error	value	error	value	error	value	error	value	error	value	error	value	error		
First reduced	Turbospec	6070	9	3.95	0.01	0.16	0.01	0.03	0.02	1.45	0.01	5.05	empirical	3.98	0.03	4.08	0.0218
	Synthe	6082	11	3.90	0.02	0.15	0.01	0.13	0.01	1.45	0.01	5.19	empirical	3.92	0.05	4.31	0.0224
	MOOG	6198	10	4.09	0.01	0.23	0.01	0.13	0.02	1.46	0.01	5.25	empirical	3.83	0.04	4.29	0.0224
Second reduced	Turbospec	6126	15	4.04	0.02	0.19	0.01	0.08	0.01	1.41	0.01	5.07	empirical	3.92	0.05	2.86	0.0206
	Synthe	6174	15	3.95	0.01	0.20	0.01	0.17	0.02	1.48	0.02	5.44	empirical	3.52	0.08	3.24	0.0219
	MOOG	6266	15	4.11	0.02	0.27	0.01	0.12	0.02	1.48	0.01	5.48	empirical	3.48	0.07	3.09	0.0213

Table B.5: Results obtained for WASP-101 with the first reduced line list (top table) and for the second reduced line list (bottom table).

		T_{eff} (K)		$\log(g)$ (dex)		$[Fe/H]$ (dex)		$[\alpha/Fe]$ (dex)		ξ (km/s)		v_{mac} (km/s)		$v\sin(i)$ (km/s)		χ^2	RMS
		value	error	value	error	value	error	value	error	value	error	value	error	value	error		
First reduced	Turbospec	-	-	-	-	-	-	-	-	-	-	-	-	-	-	-	-
	Synthe	-	-	-	-	-	-	-	-	-	-	-	-	-	-	-	-
	MOOG	-	-	-	-	-	-	-	-	-	-	-	-	-	-	-	-
Second reduced	Turbospec	6599	46	4.48	0.05	0.26	0.02	-0.01	0.05	1.64	0.05	6.39	empirical	12.32	0.13	1.01	0.0122
	Synthe	-	-	-	-	-	-	-	-	-	-	-	-	-	-	-	-
	MOOG	6707	42	4.56	0.04	0.33	0.02	-0.06	0.07	1.68	0.05	6.87	empirical	12.17	0.13	1.12	0.0129

Table B.6: Results obtained for WASP-190 with the first reduced line list (top table) and for the second reduced line list (bottom table).

		T_{eff} (K)		$\log(g)$ (dex)		[Fe/H] (dex)		[α /Fe] (dex)		ξ (km/s)		v_{mac} (km/s)		$v \sin(i)$ (km/s)		χ^2	RMS
		value	error	value	error	value	error	value	error	value	error	value	error	value	error		
First reduced	Turbospec	6553	23	4.10	0.03	0.03	0.01	0.09	0.03	1.73	0.03	6.90	empirical	13.48	0.07	1.68	0.014
	Synthe	-	-	-	-	-	-	-	-	-	-	-	-	-	-	-	-
	MOOG	6735	25	4.22	0.03	0.11	0.01	0.09	0.04	1.81	0.03	7.71	empirical	13.2	0.07	1.71	0.0141
Second reduced	Turbospec	6680	38	4.34	0.05	0.10	0.02	-0.03	0.04	1.66	0.04	7.15	empirical	13.52	0.08	1.11	0.0128
	Synthe	-	-	-	-	-	-	-	-	-	-	-	-	-	-	-	-
	MOOG	6905	29	4.37	0.03	0.20	0.02	0.08	0.04	1.9	0.03	8.53	empirical	13.15	0.11	1.13	0.0129